infrastructures

MDPI

Article

Beyond Mass Loss: Residual Flexural Strength as an Indicator for Concrete Durability in Sulfuric Acid and Sewage Environments

Hatem Affes * and Salem Georges Nehme

Department of Construction Materials and Technologies, Faculty of Civil Engineering, Budapest University of Technology and Economics, Műegyetem rkp. 3., H-1111 Budapest, Hungary; salem.nehme@emk.bme.hu
* Correspondence: affeshatem@edu.bme.hu

Abstract

Current industry standards for evaluating concrete durability in wastewater environments, such as ASTM C267, rely almost exclusively on mass loss as the primary performance indicator. This study demonstrates that mass change alone can be an ambiguous metric that does not fully characterize the structural degradation of advanced cementitious binders. Through a comprehensive physical, chemical, and mechanical evaluation of 27 binary and ternary mixtures (totalling 486 specimens), we identify four limitations of mass-based standards: **(1) The Slag Anomaly**, where excellent surface mass preservation masks a significant loss of internal structural capacity, indicating potential internal structural softening. **(2) The Sewage Anomaly, where specimens in active biogenic environments exhibit mass gain** (up to +1.21%) despite continuous chemical attack. **(3) Non-Linear Scaling**, where 5% "accelerated" acid tests fundamentally alter degradation kinetics compared to realistic 1% environments. **(4) The Maturation Conflict**, where extended curing (56 days) significantly improves the physical resistance of slow-reacting pozzolans (cyment) while increasing the mass loss of high-performance ternary blends (MK/SF), likely linked to the exhaustion of their chemical buffering capacity. Current standards relying solely on mass loss may not capture internal degradation in slag-based cements that remain geometrically intact. We propose residual flexural strength as a necessary complementary metric.

Keywords: biogenic sulfuric acid; residual flexural strength; mass loss; ternary blends; durability

1. Introduction

The rapid expansion of global urbanization has placed unprecedented pressure on wastewater treatment infrastructure. Concrete, despite being the most widely used material for sewer networks, is inherently vulnerable to the aggressive environment of wastewater systems, specifically Microbially Induced Corrosion (MIC). Recent estimates suggest that the repair and replacement of sewage systems due to biogenic sulfuric acid attack account for billions of euros annually in the EU and US alone [1,2]. Furthermore, as aging infrastructure confronts shifting wastewater compositions, elevated effluent temperatures, and longer retention times, the severity of MIC is projected to escalate, demanding more resilient and heavily optimized material solutions [3].

The degradation mechanism in these environments is distinct from classical acid attack. In the bacteriogenic cycle, *Thiobacillus* bacteria colonize the sewer crown, converting hydrogen sulphide gas (H_2S) into sulfuric acid (H_2SO_4) [4]. This process is highly dynamic and multi-staged; as the surface pH drops due to initial abiotic carbonation and H_2S

Check for updates

Academic Editors: Dayou Luo and Kejin Wang

Received: 26 March 2026
Revised: 21 April 2026
Accepted: 30 April 2026
Published: 14 May 2026

Copyright: © 2026 by the authors. Licensee MDPI, Basel, Switzerland. This article is an open access article distributed under the terms and conditions of the Creative Commons Attribution (CC BY) license.

absorption, a succession of increasingly acidophilic microbial strains accelerates the acid production, ultimately driving the pH on the concrete surface below 2.0 [5].

This biogenic acid reacts with the cementitious matrix—primarily calcium hydroxide ($Ca(OH)_2$) and calcium silicate hydrate (C-S-H)—to form expansive products such as gypsum ($CaSO_4 \cdot 2H_2O$) and ettringite [6]. These reaction products lead to surface scaling, loss of alkalinity, and eventually, the structural collapse of the pipe walls.

Despite the severity of this threat, current design and testing standards remain surprisingly prescriptive rather than performance based [7]. European Standard **EN 206** [8] efines Exposure Class XA3 for highly aggressive chemical environments but primarily mandates limiting the water-to-cement (w/c) ratio and using sulphate-resisting cements (e.g., CEM III/B). It does not, however, mandate a specific performance test to verify durability [8]. While limiting the w/c ratio effectively enhances the overall physical density of the matrix, prescriptive approaches frequently fail to capture the complex, long-term chemical buffering capacities and microstructural vulnerabilities of modern multi-component binders [9].

When performance testing is conducted, the industry predominantly relies on standards such as **ASTM C267** [10] ("Standard Test Methods for Chemical Resistance of Mortars, Grouts, and Monolithic Surfacing's"). This protocol focuses almost exclusively on **mass loss** as the primary indicator of failure. The underlying assumption is that chemical resistance is synonymous with material retention: if the concrete does not dissolve, it is assumed to be durable [10].

This study posits that mass loss, when used in isolation, is an incomplete metric for modern high-performance concrete binders. The degradation of cementitious materials is not limited to surface erosion (which reduces mass). A parallel can be drawn to marine degradation mechanisms: just as aggressive environmental chloride ions can migrate through microscopic crack networks and induce severe internal reinforcement corrosion long before macroscopic surface spalling is evident [11,12], biogenic sulfuric acid attack frequently operates on a hidden internal front.

It is hypothesized to also involve chemical alteration of the pore solution and "internal softening," where the acid penetrates the matrix and decalcifies the C-S-H gel without immediately causing material detachment [10,13–15].

In such scenarios, a concrete specimen—particularly those containing additives like blast furnace slag or metakaolin—may retain its geometric mass while suffering a significant loss of mechanical cohesion. These latent hydraulic and pozzolanic materials often produce dense, silica-rich reaction products that inherently resist dissolution, creating a deceptive gravimetric and physical stability even as the load-bearing calcium framework is depleted [16]. Conversely, a mix might experience high surface erosion (high mass loss) but maintain a dense, impenetrable core that retains structural load-bearing capacity.

Recent state-of-the-art reviews emphasize the urgent need to develop standard testing methods that capture all aspects of Microbiologically Influenced Concrete Corrosion (MICC), as a clear relationship between laboratory corrosion rates and true site behaviour remains poorly established [17]. Furthermore, recent studies stress that biogenic acid deterioration involves complex microbial interactions that significantly differ from the mechanisms of pure chemical sulfuric acid attack [18]. Long-term laboratory-field assessments comparing mass loss and mechanical properties confirm that evaluating degradation requires a multi-metric approach to avoid misinterpreting binder performance under varying exposure conditions [19].

To address this gap, this research evaluates the durability of 27 distinct concrete mix designs, including ternary blends optimized with metakaolin and silica fume, under three exposure conditions: 5% sulfuric acid (accelerated), 1% sulfuric acid (realistic), and

raw municipal sewage. The primary objective is to decouple the relationship between physical erosion and mechanical failure. By correlating mass loss data with residual flexural strength, this study aims to demonstrate that incorporating residual mechanical capacity provides a more comprehensive prediction of service life in XA3 environments, thereby proposing a complementary testing methodology that successfully aligns empirical laboratory observations with structural field realities.

2. Materials and Methods

2.1. Materials

To evaluate the durability of cementitious systems under aggressive acidic conditions, two primary cement types were used in this study in accordance with EN 197-1 and three distinct additives were employed to create binary and ternary blends (Table 1).

- CEM I 32.5 N-LH: A low-heat Ordinary Portland Cement (Duna-Dráva Cement Kft., Vác, Hungary) used as the reference binder.
- CEM III/B 32.5 N-LH/SR: A sulphate resisting blast furnace cement (Duna-Dráva Cement Kft., Vác, Hungary) containing high slag content, selected for its theoretical resistance to chemical attack.
- Metakaolin (MK): High-purity flash-calcined metakaolin Metaver® I, NEWCHEM GmbH, Baden, Austria) was used as a type II latent hydraulic additive. It is characterized by an amorphous aluminosilicate structure with a silica (SiO_2) content of 52–54% and alumina (Al_2O_3) content of 43–44%. The material possesses a median particle size (d_{50}) of <7–9 μm and a particle density of 2.6 g/cm^3 and a specific surface area (BET) of approximately 18 m^2/g.
- Silica Fume (SF): Densified silica fume (SikaFume® HR/TU, Sika Hungária Kft., Biatorbágy, Hungary) was used as a micro-filler and pozzolan. The particles are non-crystalline with a typical diameter of ≈0.1 μm, a particle density of approximately 2.3 g/cm^3 (at 20 °C) and a bulk density of 0.65 kg/dm^3, compliant with EN 13263-1. The SF was used to enhance internal cohesion, reduce water permeability, and improve the chemical resistance of the hardened concrete through its reaction with free lime ($(CaOH)_2$) to form additional C-S-H phases.

Table 1. Additives technical description.

Material	Commercial Name	Particle Density (g/cm^3)	Specific Surface (Blaine)
Metakaolin	Metaver™ N	2.6	≈22.000 cm^2/g
Silica Fume	SikaFume® HR/TU	2.3	0.1 μm (Avg. Particle)
Volcanic Tuff	cyment® L 100	2.45	≥10.000 cm^2/g

Mechanically Activated Volcanic Tuff (cyment Kft, Mosonmagyaróvár, Hungary): A high-performance, mechanically activated natural pozzolan (cyment® L 100) was used as a reactive mineral addition. This material is a vitric phonolitic tuff with a high amorphous aluminosilicate content. It is characterized by an exceptionally high fineness, processed to a specific surface area (Blaine) of ≥10,000 cm^2/g, which is significantly higher than standard cement. The material has a particle density of 2.45 ± 0.05 g/cm^2 and a bulk density (loose) of 0.60–0.90 g/cm^3. Due to its extreme fineness ($d_{95} \leq 10$ μm), it acts both as a high-reactivity pozzolan and a micro-filler, significantly increasing the packing density and chemical resistance of the cementitious matrix.

2.2. Mix Design and Optimization Strategy

A total of 27 concrete mixtures were designed to investigate the synergistic effects of binary and ternary binder systems on microstructural densification and chemical resistance. The experimental program focused on six groups of concrete detailed in Table 2 and four primary groups.

Table 2. Complete Mix Design Matrix.

Mix ID	Binder Composition	Binder Components (kg/m^3)	*w/c* Ratio	Relative SP Dosage (To Total Binder) in %	Fresh Density (kg/m^3)	Flow Table (mm)/Consistency Class
Reference—Group 1						
H1	CEM I	Cement: 330	0.50	0.43	2348	510 mm/F4
H3	CEM I	Cement: 360	0.40	1.76	2435	520 mm/F4
H16	CEM I	Cement: 360	0.50	0.28	2312	420 mm/F3
H24	CEM I	Cement: 360	0.40	1.11	2398	520 mm/F4
H2	CEM III/B	Cement: 330	0.50	0.81	2401	500mm/F4
H4	CEM III	Cement: 360	0.40	0.28	2362	530 mm/F4
CEM I + cyment—Group 2						
H10	CEM I + Cy	Cement: 323, cyment: 57	0.50	0.96	2390	510 mm/F4
H11	CEM I + Cy	Cement: 266, cyment: 114	0.50	2.58	2436	460 mm/F3
H12	CEM I + Cy	Cement: 323, cyment: 57	0.45	1.84	2401	420 mm/F3
H13	CEM I + Cy	Cement: 266, cyment: 114	0.45	1.05	2383	530 mm/F4
H14	CEM I + Cy	Cement: 266, cyment: 114	0.50	0.74	2377	530 mm/F4
Metakaolin—Group 3						
H17	CEM I + MK	Cement: 324, MK: 36	0.50	0.39	2316	455 mm/F3
H22	CEM I + MK	Cement: 324, MK: 36	0.40	0.17	2410	350 mm/F2
Silika Fume—Group 4						
H19	CEM I + SF	Cement: 324, SF: 36	0.50	0.41	2275	490 mm/F3
H25	CEM I + SF	Cement: 324, SF: 36	0.40	0.61	2354	400 mm/F2
H27	CEM I + SF	Cement: 324, SF: 36	0.50	0.28	2342	500 mm/F4
CEM III/B + cyment—Group 5						
H15	CEM III/B + Cy	Cement: 323, cyment: 57	0.50	1.92	2340	600 mm/F5
H30	CEM III/B + Cy	Cement: 266, cyment: 114	0.50	1.72	2333	535 mm/F4
H31	CEM III/B + Cy	Cement: 323, cyment: 57	0.45	1.60	2352	595 mm/F5
H32	CEM III/B + Cy	Cement: 266, cyment: 114	0.45	1.87	2333	455 mm/F3
Ternary Blends—Group 6						
H18	CEM I + MK + SF	Cement: 324, MK: 18, SF: 18	0.50	0.39	2308	460 mm/F3
H20	CEM I + MK + SF	Cement: 306, MK: 36, SF: 18	0.50	0.22	2292	485 mm/F3
H21	CEM I + MK + SF	Cement: 306, MK: 18, SF: 36	0.50	0.28	2286	430 mm/F3
H23	CEM I + MK + SF	Cement: 324, MK: 18, SF: 18	0.40	3.8	2418	495 mm/F4
H26	CEM I + MK + SF	Cement: 306, MK: 36, SF: 18	0.40	0.69	2370	420 mm/F3
H28	CEM I + MK + SF	Cement: 324, MK: 18, SF: 18	0.50	0.28	2339	510 mm/F4
H29	CEM I + MK + SF	Cement: 306, MK: 18, SF: 36	0.40	0.83	2366	495 mm/F4

Note: Flow consistency classes were measured in accordance with European Standard EN 206 (tested in accordance with EN 12350-5).

- **References**: Pure CEM I or CEM III control mixes formulated at varying water-to-cement (w/c) ratios (0.40 and 0.50) to establish baseline performance.
- **Volcanic Tuff (cyment) Modified Group (H10–H14):** Binary blends consisting of CEM I modified with varying dosages of mechanically activated volcanic tuff (cyment® L 100) and adjusting w/c ratios.
- **CEM III/B (Slag) + Volcanic Tuff Group (H15, H30–H32):** Blends utilizing sulphate-resisting blast furnace cement (CEM III/B) modified with varying replacement percentages of cyment® L 100.
- **Metakaolin and Silica Fume Group (H17–H23, H25–H29):** High-performance binary and ternary systems incorporating CEM I, high-purity metakaolin (Metaver™ N), and densified silica fume (SikaFume® HR/TU) at various replacement ratios and w/c parameters.

River gravel and sand were used as aggregates, fractioned into 0/4 mm, 4/8 mm, and 8/16 mm sizes. To achieve adequate workability in high-fines ternary mixes, a polycarboxylate ether (PCE) based superplasticizer (MasterGlenium® 300) was employed. This admixture has a solid content of 44% and a density of 1.1 g/cm^3.

A targeted workability approach was employed to ensure adequate compaction and microstructural consistency across the mix designs. The initial target consistency was set to the F3 flow class for reference mixes and F4 for high-fines blends to ensure proper dispersion without increasing the w/c ratio. The dosage of the polycarboxylate ether (PCE) superplasticizer was adjusted experimentally.

However, due to the extreme specific surface areas of the supplementary cementitious materials—specifically the Metaver™ N (≈~22,000cm^2/g) and SikaFume® HR/TU (≈0.1 μm)—the mixtures exhibited immense water demand and rapid stiffening. When PCE dosages were kept minimal (e.g., H22 at 0.17%), workability was severely restricted to the F2 flow class. To overcome this immense internal surface area and achieve the target F3 or F4 consistency in other high-replacement blends (e.g., H11, H23), the superplasticizer dosage had to be pushed to extreme levels (2.58% and 3.8%, respectively), far exceeding standard manufacturer recommendations.

Conversely, when these additives were combined with optimized superplasticizer ratios and adequate water content (e.g., H15, H31), the mixtures exhibited extreme fluidity, reaching the F5 flow class (up to 600 mm). In these instances, the availability of sufficient free water and PCE allowed the superplasticizer to fully deflocculates the fine particles, pushing the paste toward self-compacting characteristics.

2.3. Specimen Preparation and Curing

To ensure microstructural homogeneity and eliminate the "wall effect" (cement-rich surface skin) associated with individually cast small prisms, specimens were fabricated using a bulk-casting and sectioning method. For each mix design, standard cubic monoliths (150 × 150 × 150 mm) were cast in steel moulds and compacted via a vibrating table to eliminate entrapped air. After 24 h, the specimens were demoulded and cured underwater at 20 ± 2 °C for 7 days in a lime-saturated water bath, followed by standard laboratory curing until their designated testing age.

A dual-age testing approach (28 and 56 days) was deliberately selected prior to cutting and chemical exposure to account for the slow hydration kinetics of the diverse binder systems. Because the mix designs heavily incorporate latent hydraulic materials and pozzolans, exposing these high-replacement blends to aggressive acid at the conventional 28-day mark evaluates an immature microstructure. The prolonged 56-day maturation period provided the secondary hydration reactions the extended duration necessary to

fully consume the available Portlandite ($Ca(OH)_2$) and densify the capillary pore network, thereby reflecting the true long-term chemical resistance of the concrete in service.

At the maturation ages of 28 and 56 days, the hardened cubes were sectioned using a water-cooled diamond saw to produce the final prismatic test specimens (50 × 50 × 150 mm) (±2 mm). This preparation method served two purposes. First, it exposed the internal aggregate–paste matrix directly to the aggressive environment, preventing the artificial delay of chemical attack often caused by the protective laitance layer on cast surfaces. Second, it ensured that all replicate prisms for a given mix originated from the exact same compaction batch, strictly minimizing intra-sample variability.

2.4. Chemical Exposure Protocols

At the maturation ages of 28 and 56 days, a total of 486 specimens were transferred to three distinct aggressive environments for a duration of 6 weeks. These environments (Figure 1) were specifically designed to simulate varying degrees of biogenic sulfuric acid (BSA) attack and microbiological induced corrosion (MIC). For each mix design, 18 prisms were evaluated: 3 control specimens submerged in water, 6 specimens in 5% acid (3 static, 3 brushed), 6 specimens in 1% acid (static), and 3 specimens in raw wastewater.

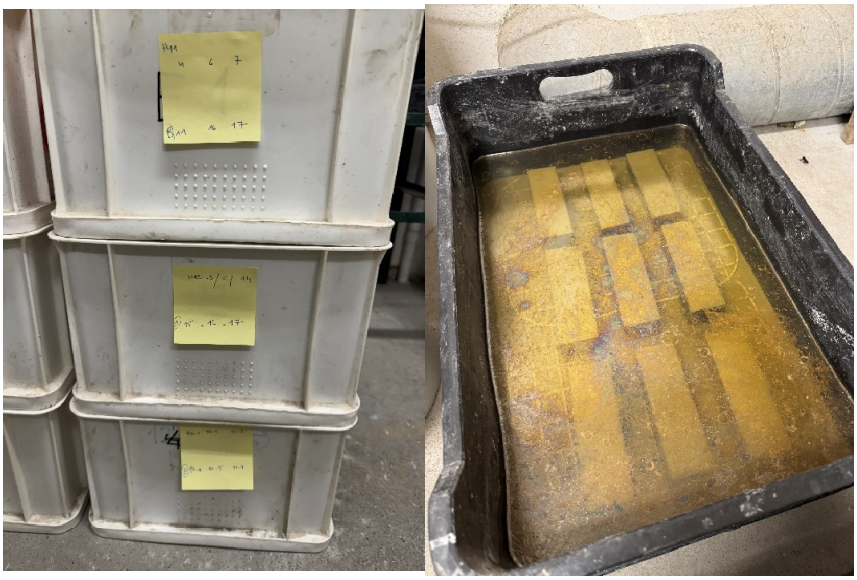

Figure 1. Photos of the Acid and the sewage bath setups.

For each exposure condition and testing age, specimens were evaluated in triplicate (n = 3) originating from the same batch. All gravimetric and mechanical results reported herein represent the arithmetic mean of these three replicate specimens, with the standard deviation provided to indicate intra-batch variability.

To simulate extreme biogenic corrosion and accelerate degradation kinetics, specimens were immersed in a 5% (w/w) sulfuric acid solution. The fresh acid bath possessed an initial, highly aggressive pH of approximately 0.2. During each 7-day immersion cycle, the acid reacted with the alkaline cementitious matrix, gradually neutralizing. Measurements recorded immediately prior to the weekly renewal of the solution yielded pH values typically between 0.60 and 0.90. This condition was divided into two sub-groups: a static group where specimens remained undisturbed, and a brushed group where softened reaction products were mechanically removed weekly using a wire brush to simulate the erosive flow of wastewater.

To simulate the most aggressive, naturally occurring chemical conditions of the sewer crown, specimens were immersed in a 1% (w/w) sulfuric acid solution. This concentration

permits the natural formation of a gypsum diffusion barrier within the pore network, preventing artificial "total dissolution" and reflecting field degradation kinetics. The freshly prepared solution possessed an initial pH of 0.8 to 0.9. As the hydrogen ions were gradually consumed by the matrix, the solution neutralized to pH values between 1.0 and 1.2 prior to the weekly renewal.

To evaluate performance under actual Microbiologically Induced Corrosion (MIC), an ex situ immersion test was established using raw municipal influent. The wastewater was collected directly from a closed municipal influent channel at the Budapest University of Technology and Economics (BME) in Budapest, Hungary. The concrete specimens were immersed in static incubation tanks within a controlled laboratory environment, maintained at an ambient temperature of 20 ± 2 °C. To ensure a continuous supply of nutrients and active microbial colonies to the otherwise stagnant baths, the wastewater solution was entirely replenished every 7 days with freshly collected influent. Throughout the exposure period, the pH of this highly active bacteriogenic environment fluctuated dynamically between 1.2 and 3.5.

2.5. Testing Methods

2.5.1. Mass Loss and Visual Inspection

Prior to chemical exposure, all prismatic specimens were conditioned in a laboratory oven at 60 degrees for 24 h to establish a definitive, initial oven-dry mass (M_0).

To continuously track physical degradation, specimens were extracted from their respective exposure environments at 7-day intervals. Upon removal, a strict handling protocol was implemented to ensure measurement consistency without disturbing the fragile corrosion layers. Specimens exposed to the static 1% acid and raw sewage environments were gently rinsed with distilled water to remove loose debris, then carefully patted to a saturated-surface-dry (SSD) condition using a damp absorbent cloth. This deliberate, low-impact drying method was employed to preserve the accumulated organic biofilm and soft gypsum layers (Figure 2), preventing artificial mass reduction prior to weighing. Conversely, specimens in the brushed 5% acid group were mechanically scrubbed under running water to remove all reaction products before being brought to the SSD condition.

Once in SSD condition, each prism's weekly intermediate mass (M_t) was weighed using a precision digital laboratory scale accurate to 0.1 g. At the conclusion of the 6-week testing period, a final gravimetric measurement was conducted once again conditioning all specimens in a 60 degree oven for 24 h to record their final dry mass.

The cumulative mass change percentage at any given exposure week (t) was calculated relative to the specimen's initial, uncorroded oven-dry mass (M_0), using the following formula:

$$M_t(\%) = \frac{M_t - M_0}{M_0} \times 100$$

A negative value indicates material erosion (mass loss), whereas a positive value indicates the absorption of liquids or the accumulation of biological matter (mass gain). This precise tracking was essential for later correlating physical mass variations with residual structural capacity.



Figure 2. Specimen degradation.

2.5.2. Ph Monitoring and Neutralization Rate

The pH of the bulk acidic immersion solutions (the liquid actively surrounding the prismatic concrete specimens) was monitored weekly using a calibrated digital pH meter (Testo 206, Testo SE & Co. KGaA, Titisee-Neustadt, Germany). Measurements were taken directly from the incubation tanks immediately prior to the scheduled weekly solution renewal. In this closed exposure system, a rise in the solution's pH indicates the active neutralization of the acid. In this specific context, "neutralization" refers to the continuous chemical consumption of hydrogen ions (H^+) from the sulfuric acid by hydroxyl ions (OH^-) released from the cementitious matrix. This ion exchange is driven primarily by the dissolution and outward leaching of highly soluble, alkaline Portlandite ($Ca(OH)_2$).

Consequently, maintaining a lower solution pH (closer to the initial acidic baseline) over the 7-day cycle indicates a reduction in the overall chemical reactivity of the concrete. For the binary and ternary blends evaluated in this study, tracking this macroscopic neutralization rate serves as a proxy to quantify the effectiveness of the pozzolanic additions (metakaolin and volcanic tuff). A lower neutralization rate demonstrates their capacity to consume vulnerable free lime during the prior maturation period, thereby restricting the availability of the acid's primary reactant during exposure. Residual Flexural Strength.

2.5.3. Residual Flexural Strength

Unlike standard evaluation protocols that rely solely on physical mass loss, this study prioritized post-corrosion structural integrity as the definitive metric of durability. Mass loss measurements inherently fail to capture internal microstructural degradation, such as the deep decalcification and internal softening observed in slag-based matrices. Therefore, following the 6-week exposure regimens, the 50 × 50 × 150 mm prismatic specimens—many of which exhibited severe macroscopic surface degradation—were subjected to a three-point bending test.

Testing was conducted using a closed-loop servo-hydraulic testing machine (Instron 600DX, Instron, Norwood, MA, USA) equipped with a 600 kN load cell. The prisms were tested over a clear span of **100 mm** at a continuous displacement rate of **0.5 mm/min** until failure.

The peak load was recorded, and the residual flexural strength was calculated. These values were then directly compared against the baseline strengths of non-corroded reference specimens of identical age to determine the "Strength Retention Factor." This mechanical evaluation provided a definitive assessment of the core integrity of the ternary blends, effectively isolating true microstructural acid resistance from superficial surface erosion.

Due to the severe surface erosion and non-uniform mass loss observed in several mixtures (specifically the H10 reference and high-volume cyment blends), the prismatic specimens exhibited significant geometric irregularities. During the three-point bending tests, these surface 'craters' and degraded zones created loading eccentricities, occasionally leading to minor specimen rotation or 'twisting' during the initial loading phase. To mitigate this, a specialized self-aligning support system was utilized, and the crosshead displacement was maintained at a strictly controlled 0.5 mm/min to allow the internal load-bearing core to stabilize before ultimate failure.

3. Results Phase I: Limitations of Gravimetric Assessment

Standardized testing protocols for concrete durability traditionally prioritize physical mass loss as the definitive metric for chemical resistance. However, continuous gravimetric monitoring across the three distinct exposure environments (accelerated 5% H_2SO_4, realistic 1% H_2SO_4, and raw municipal sewage) revealed profound limitations in this conventional approach.

The data demonstrates that mass change is a highly inconsistent metric in biogenic sulfuric acid (BSA) scenarios. Specifically, the accumulation of expansive corrosion products (such as gypsum and ettringite) in static acid baths, coupled with the absorption of liquids and organic biofilms in raw sewage, frequently triggers an artificial mass stabilization or even a net mass gain. This superficial mass retention masks the probable onset of deep microstructural decalcification and internal softening. Consequently, the results below in Table 3 indicate that relying solely on gravimetric surface erosion rates does not fully capture the true residual structural capacity of wastewater infrastructure presented in Table 4.

Table 3. Average Mass Change (%) After 6 Weeks of Exposure—All unbrushed categories.

Mix ID	5% Acid	1% Acid	Raw Sewage	Water Control
Start of Acid exposure: 28—day				
H16	−34.07 ± 0.50	−3.20 ± 0.46	−0.69 ± 0.03	−0.81 ± 0.08
H10	−33.80 ± 0.84	−4.99 ± 0.99	0.41 ± 0.07	0.45 ± 0.12
H15	−21.86 ± 1.46	−2.09 ± 0.25	−1.42 ± 0.04	−1.12 ± 0.06
H22	−30.92 ± 0.35	−6.26 ± 0.78	−0.97 ± 0.15	+0.39 ± 0.08
Start of Acid exposure: 56—day				
H16	−33.57 ± 1.00	−2.19 ± 0.77	1.21 ± 0.34	0.72 ± 0.46
H10	−29.04 ± 2.16	−4.27 ± 0.87	0.93 ± 0.14	0.66 ± 0.12
H15	−19.17 ± 0.48	−1.47 ± 0.15	0.72 ± 0.19	0.48 ± 0.28
H22	−36.50 ± 2.07	−5.70 ± 0.21	−2.14 ± 0.50	0.21 ± 0.14

Note: All values represent the arithmetic mean of three replicate specimens (n = 3) ± the standard deviation. Negative values indicate mass loss (erosion); positive values indicate mass gain (absorption/accumulation). The data format is [Mean] ± [SD].

Table 4. Residual Flexural Strength and Strength Retention.

Mix ID	Unexposed Control Strength (MPa)	5% Acid Exposed Strength (MPa)	Strength Retention Factor (%)
Start of Acid exposure: 28—day			
H16	8.44 ± 1.01	6.61 ± 2.01	78.3%
H10	11.70 ± 1.45	10.48 ± 1.80	89.6%
H15	6.44 ± 0.52	4.39 ± 0.83	68.2%
H22	13.65 ± 1.25	11.34 ± 0.33	82.85%
Start of Acid exposure: 56—day			
H16	8.54 ± 0.96	7.99 ± 2.20	93.5%
H10	12.18 ± 1.41	11.28 ± 1.30	92.7%
H15	6.80 ± 0.96	5.17 ± 0.89	76.0%
H22	13.86 ± 0.07	11.35 ± 1.49	81.9%

Note: Flexural strength values represent the mean peak load capacity of three replicate specimens (n = 3) ± standard deviation. The Strength Retention Factor is calculated using the respective mean values. The data format is [Mean] ± [SD].

3.1. Accelerated Degradation in 5% Sulfuric Acid

The specimens exposed to the 5% H_2SO_4 solution exhibited the classical, severe degradation mechanisms expected of cementitious materials in highly aggressive chemical environments [8,11]. The reaction kinetics were driven by the extreme initial acidity (pH ≈ 0.2), which actively consumed the alkaline paste and neutralized the surrounding solution to a pH of 0.60–0.90 by the end of each 7-day cycle.

In this accelerated erosion environment, the reference CEM I mix (H16) suffered significant deterioration, recording a severe mass loss of 34.07% at 28 days. The rapid degradation front suggests the acid aggressively dissolved the abundant Portlandite ($Ca(OH)_2$) and decalcified the primary C-S-H gel, leaving behind a structurally compromised, gypsum-rich sludge. In contrast, the high-performance binary and ternary blends—specifically the cyment-modified mix (H10) and the Metakaolin-optimized mix (H22)—demonstrated reduced mass loss under brushed conditions. This early-age resistance is theorized to stem from microstructural densification, where the forced dispersion of ultra-fine SCMs potentially created a highly tortuous pore network that restricted the inward diffusion of sulphate and hydrogen ions.

The influence of binder content on gravimetric stability was further elucidated by comparing the two reference mixtures at an identical w/c ratio of 0.50. Increasing the CEM I content from 330 kg/m^3 (H1) to 360 kg/m^3 (H16) resulted in a significant improvement in mass retention, with 28-day mass loss in 5% acid dropping from $-49.50 \pm 2.15\backslash\%$ to $-34.07 \pm 0.50\backslash\%$. This demonstrates the 'Alkaline Buffer Effect,' where the higher volume of Portlandite in the 360 kg/m^3 mix provides a more robust chemical reserve to neutralize the sulfuric acid before it can fully dissolve the structural C-S-H gel. However, the nearly identical strength retention factors between these two dosages suggest that while higher cement content delays surface erosion, the rate of internal structural softening remains fundamentally dictated by the chemical resistance of the binder type itself.

A comparative analysis of identical mixtures cured for 28 days (Figure 3a) versus 56 (Figure 3b) days prior to 5% H_2SO_4 exposure revealed a previously underreported paradox regarding pozzolanic reactivity and chemical buffering:

- **The "Slow Reactors" (cyment/Slag):** For mixtures incorporating mechanically activated volcanic tuff (cyment), extended curing significantly improved chemical resistance. For instance, the mass loss of **H10 (CEM I + cyment) dropped from 33.80% at**

28 days to 29.04% at 56 days. Because these latent hydraulic materials react slowly, they require a full 56 days to sufficiently densify the matrix and establish a protective microstructural shield.

- **The "Fast Reactors" (Metakaolin/Silica Fume):** Conversely, the hyper-reactive ternary blends exhibited increased vulnerability at 56 days. **The H22 (Metakaolin) mass loss increased from 30.92% at 28 days to 36.50% at 56 days.**

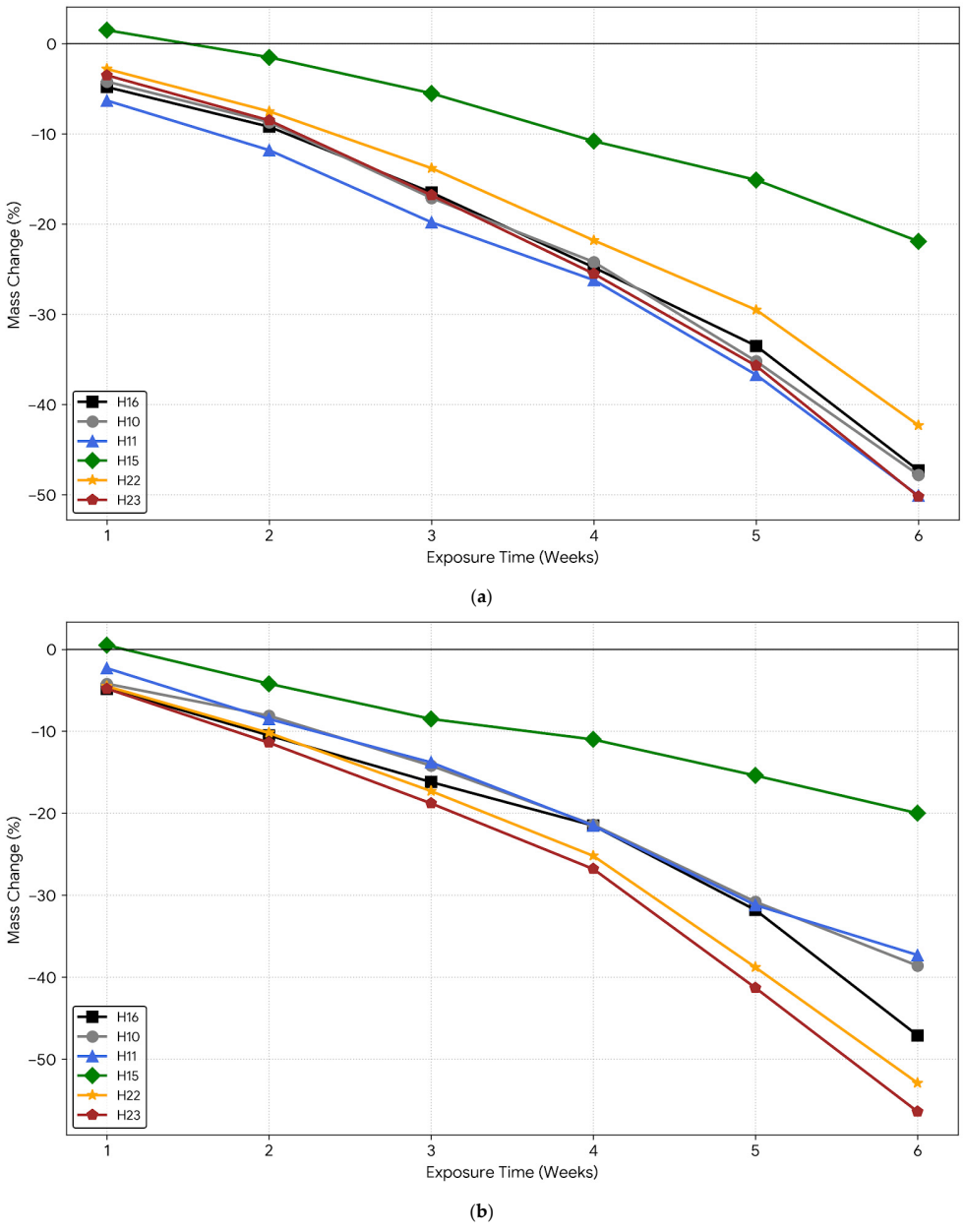

Figure 3. (**a**) Mass change in 5% H_2SO_4 at 28-day curing. (**b**) Mass change in 5% H_2SO_4 at 56-day curing.

Comparing the 28-day and 56-day curing performances reveals distinct chemical mechanisms at play. The baseline Pure CEM I (H16) maintained a stable degradation profile due to a lack of late-stage pozzolanic reactions. Conversely, the hyper-reactive Metakaolin blends (e.g., H22) suffered from the exhaustion of their Portlandite buffering capacity, leading to increased structural vulnerability. In contrast, the slow-reacting tuff blends (e.g., H10) demonstrated improved resistance over time due to late-age microstructural densification.

This paradox identifies a fundamental flaw in extreme acid testing. Mechanical data suggests that Metakaolin and Silica Fume are so efficient that, by 56 days, they may have consumed a vast majority of the available Portlandite via the pozzolanic reaction. In a 5% acid bath, Portlandite acts as a necessary "sacrificial buffer"—it neutralizes the acid before it can attack the structural C-S-H gel. It appears that because the 56-day MK/SF matrices lacked this free lime buffer, the acid attacked the main structural network more rapidly.

3.2. The Non-Linearity of Realistic Exposure (1% H_2SO_4)

When exposed to the 1% H_2SO_4 solution—a concentration more representative of severe biogenic corrosion in active sewer crowns (pH ≈ 1.0–1.2)—the degradation mechanisms did not simply slow down; they fundamentally altered. The H16 reference mix recorded a mass loss of only 2.19% after 6 weeks (at 56 days curing), compared to nearly 33.5% in the 5% solution.

More importantly, in this lower acidity, several high-performance advanced mixes (such as the slag-based H15) exhibited minimal mass loss (−1.47%) or even artificial stabilization. At 1% concentration, the acidity is insufficient to wash away the reaction products. The specimens absorb the liquid and grow a dense layer of gypsum and ettringite within their pores. Because this layer is not dissolved, the concrete gains physical weight. Consequently, reliance on mass loss data from 1% acid exposure yields statistically ambiguous results across different high-performance mixes, failing to distinguish between superior durability and inconsistent liquid absorption.

This realistic environment highlights three distinct stability profiles. The baseline CEM I (H16) undergoes slow surface erosion where gypsum wash-off slightly outpaces absorption. The Slag blends (e.g., H15) exhibit a "Gypsum Barrier Effect," where low acidity allows reaction products to precipitate within pores, artificially stabilizing physical mass. Finally, the Metakaolin blends (H22) achieve structural core preservation through chemical starvation; their highly efficient Portlandite consumption restricts acid ingress, even while mass gain masks the slow chemical attack.

3.3. Mass Retention in Raw Sewage Environments

The most definitive finding regarding the limitations of mass loss protocols emerged from the raw municipal wastewater exposure. Despite the environment being actively acidic (pH fluctuating dynamically between 1.2 and 3.5), the specimens did not exhibit mass loss. Instead, the reference specimens (H16) and the cyment blends (H10) displayed a continuous mass gain of +1.21% and +0.93% respectively over the 56-day exposure period.

This "negative erosion" phenomenon is driven by pore saturation and organic clogging. The porous structure of the concrete absorbed the liquid phase of the wastewater, and a layer of organic sludge and biofilm accumulated on the surface [4,20], which could not be fully removed without damaging the fragile concrete skin during gravimetric measurement. This highlights the fundamental failure of current standards: a strictly mass-based evaluation would categorize these mixes in raw sewage as "chemically unchanged" or even "improved". In reality, continuous pH monitoring confirmed the environment was highly aggressive.

Figure 4 shows the contrast between exposure type and mass loss and highlights the fundamental failure of current standards: a strictly mass-based evaluation would categorize the H10 mix in raw sewage as "chemically unchanged" or even "improved" (due to apparent density gain). In reality, continuous pH monitoring confirmed the environment was highly aggressive. This proves conclusively that in realistic XA3 environments containing organic matter, physical mass change is an inconsistent metric that masks the onset of chemical attack and liquid ingress.

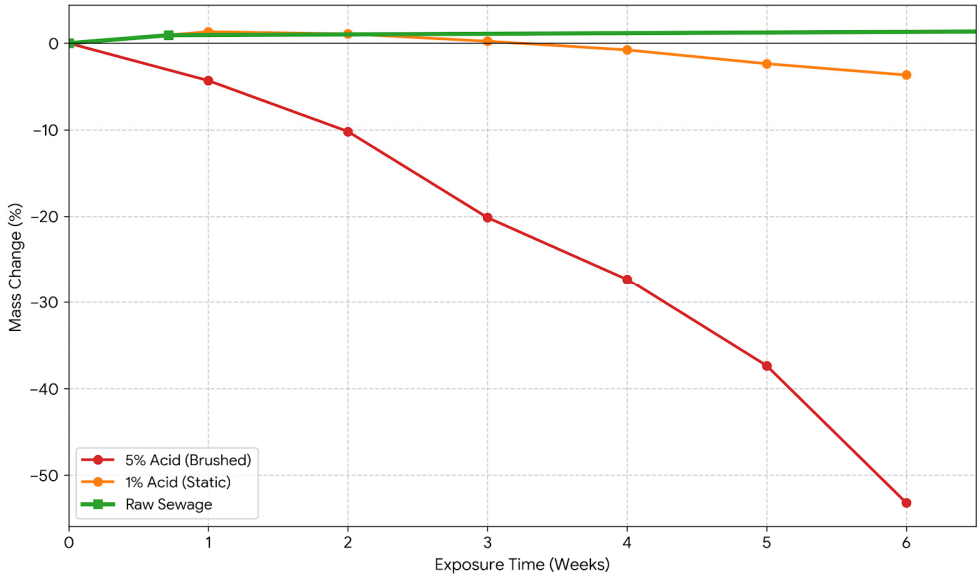

Figure 4. Mass Change (%) over Time Across All Exposure Environments—Mix H10.

4. Results Phase II: Chemical Reactivity

To understand the chemical mechanism driving the mass loss, the pH evolution of the immersion solutions was monitored (Figure 5). A rise in solution pH indicates the consumption of acid (H^+ ions) by the cementitious matrix (neutralization), which directly correlates with the rate of chemical deterioration.

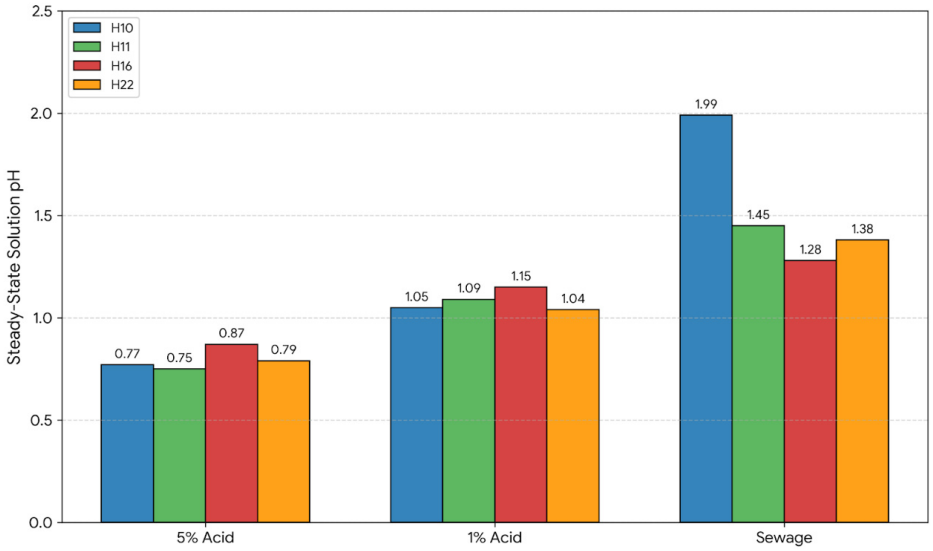

Figure 5. Week 6 pH neutralization (28 day).

4.1. Initial Surface Shock and Steady-State Degradation (5% H_2SO_4)

During the first week of exposure, both systems exhibited a rapid, highly reactive neutralization phase. The solution's pH rose sharply from the initial baseline to 2.32 for H16 and 2.65 for H22. This immediate spike indicates the rapid dissolution of the uncarbonated, calcium-rich surface layer, where the abundant free lime violently reacted with the acid to form the initial gypsum crust.

Following this initial surface shock, the degradation kinetics shifted. As shown in Figure 6, the weekly neutralized pH values for both mixes dropped and stabilized within the 0.60–0.90 range. This "steady-state" acidity confirms that the highly concentrated 5%

acid bath provided an effectively infinite supply of hydrogen ions, ultimately overwhelming the natural alkaline buffering capacity of the concrete matrices regardless of binder type.

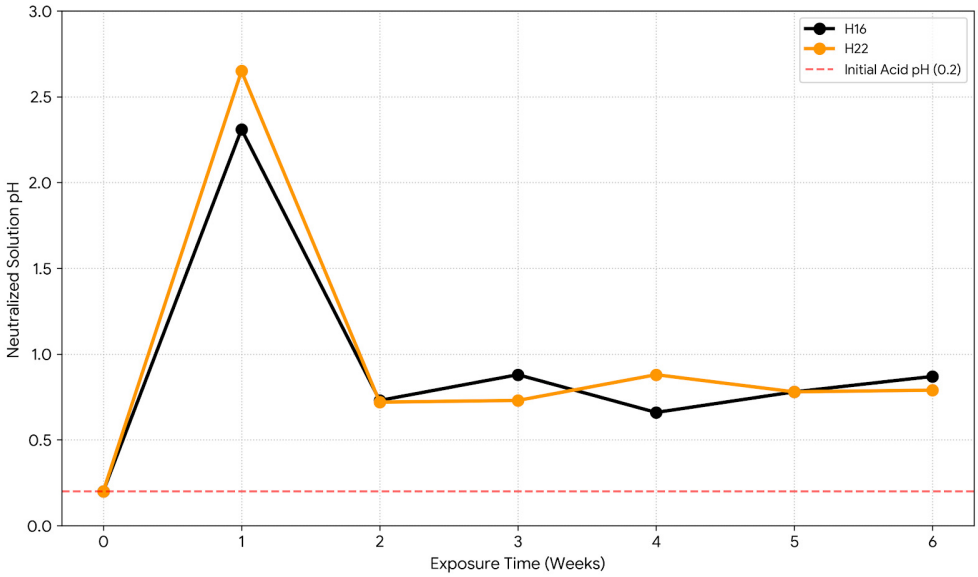

Figure 6. pH Neutralization Curve for the reference mixes (H16 and H22).

4.2. The Buffering Limit (1% H_2SO_4)

While the 5% acid overwhelmed all samples, the chemical superiority of the additive-optimized blends became clearly quantifiable in the realistic 1% acid environment. Under these field-representative conditions, the H16 reference maintained a consistently higher average neutralized pH (1.08) compared to the H22 blend (1.19).

This 0.11 pH difference—which is highly significant on a logarithmic scale—serves as the chemical explanation for the mass loss behaviours observed in Phase I. It indicates that the Metakaolin-based matrix of H22 released substantially fewer hydroxyl ions into the surrounding solution. This measurable reduction in chemical reactivity strongly indicates that the pozzolans consumed the highly soluble Portlandite ($Ca(OH)_2$) during the 56-day maturation period. By converting the vulnerable free lime into stable C-S-H gel prior to exposure, the H22 matrix appears to have effectively "starved" the acid of its primary reactant.

4.3. Verifying the Sewage Anomaly

The pH monitoring data (Figure 7) also provides the context needed to interpret the raw sewage exposure. In Phase I, the gravimetric data suggested the reference mixes were "stable" or gaining mass in sewage. However, continuous pH tracking demonstrates that the wastewater in contact with the specimens consistently neutralized, confirming an active chemical attack. For instance, the raw sewage containing the H10 reference mix spiked from varying acidic baselines up to a steady-state pH of 1.99, while the CEM I (H16) and Metakaolin (H22) baths neutralized to 1.28 and 1.38, respectively. This active buffering confirms that hydrogen ions were continuously dissolving the alkaline matrix.

This active neutralization confirms that hydrogen ions were continuously attacking and dissolving the alkaline matrix. The discrepancy between the active chemical neutralization (Phase II) and the physical mass gain (Phase I) proves that mass-based standards fail to detect active biogenic corrosion when organic clogging and liquid absorption are present.

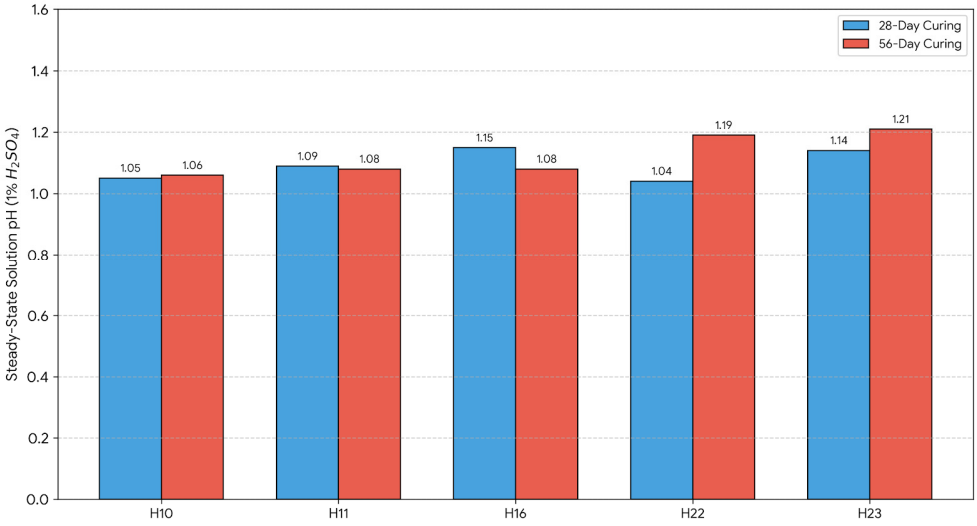

Figure 7. Week 6 pH neutralization 1% H_2SO_4 (56 day).

5. Results Phase III: Residual Flexural Strength

While mass-loss metrics frequently suggest that certain binders—particularly slag and metakaolin blends—are highly resistant to chemical attack, post-corrosion structural evaluations reveal a deeper, more concerning reality. Unlike standard protocols that rely solely on gravimetric changes (e.g., ASTM C267), this study evaluated the actual post-corrosion structural integrity via three-point bending tests. By comparing the residual flexural strength of exposed specimens against water-cured reference samples of identical age, this study defines the "Strength Retention Factor." As demonstrated below in Table 4, this mechanical evaluation highlights scenarios where physical mass diverges from load-bearing capacity, emphasizing the limitations of relying exclusively on surface-level monitoring.

5.1. The Slag Anomaly: Mass Preservation vs. Structural Softening

The most profound evidence of the "structural deception" inherent in mass-based metrics was observed in the CEM III/B + cyment blend (H15). In the accelerated 5% H_2SO_4 environment (56-day curing), H15 appeared as a top performer gravimetrically, maintaining a nearly perfect geometric profile with a mass loss of only 19.17 ± 0.48%—significantly lower than the 33.57 ± 1.00% loss recorded for the pure CEM I reference (H16). Because the silica-rich gel produced by slag hydration resists acid dissolution [19], these specimens did not exhibit the surface "craters" common in more eroded mixtures.

However, this visual and geometric stability appears to be an inconsistent indicator of the actual structural condition. Despite its stable appearance, mechanical testing revealed that H15 may have suffered severe structural compromise. Its residual flexural strength dropped to 5.17 ± 0.89 MPa, representing a Strength Retention of only 76.0%. In contrast, mixtures like H10 (CEM I + cyment) exhibited more surface erosion (29.04% mass loss) yet successfully protected their load-bearing cores to reach a superior strength of 11.28 ± 1.30 MPa (92.7% retention).

This profound strength reduction suggests that the acid successfully penetrated the H15 matrix and decalcified the C-S-H gel without causing immediate material detachment—a hypothesized process defined here as internal softening. While the specimen remained "intact" on a laboratory scale, it lacked the primary structural bonding of a healthy matrix.

5.2. Optimized Microstructures and the Maturation Effect

In stark contrast to the slag anomaly, the highly densified ternary and binary mixtures effectively protected their load-bearing cores from acid penetration, even when surface

mass was eroded. Furthermore, corresponding to the "Maturation Paradox" observed in the gravimetric data, the flexural strength results prove that waiting for 56 days before exposure radically changes the structural durability of slow-reacting mixtures:

- H10 (CEM I + cyment): Improved its strength retention in 5% acid from 89.6% (28 d cure) to 92.7% (56 d cure).
- H16 (Pure CEM I Reference): Also demonstrated mechanical resilience with extended curing, with strength retention rising from 78.3% to 93.5%.

This indicates that the 56-day curing period allows for a robust densification of the interfacial transition zone (ITZ). Even when the outer paste is actively attacked and dissolved by acid, the core structural integrity remains far superior in matured samples.

5.3. Hidden Degradation in Realistic Environments (1% Acid and Sewage)

In the realistic 1% acid and raw sewage environments, structural integrity remained universally high (85–100% retention) across all mixtures, further proving the disconnect between mass and strength. Most notably, for the H10 reference mix in raw sewage, the inconsistent mass gain of +0.93% (caused by liquid ingress and biofilm accumulation) was paired with a high strength retention of 94.39%. This indicates that while the active biogenic environment was neutralizing the surface and artificially increasing the physical weight of the specimen, the chemical degradation front had not yet penetrated deep enough to compromise the load-bearing core.

6. Discussion

6.1. Divergences Between Mass Loss and Structural Integrity

As established in the mechanical evaluation, the assumption that mass loss strictly correlates with structural performance is not consistently valid across all modern ternary and binary blends. The data highlights three distinct pathways where mass loss provides incomplete indicators of service life:

- The Slag Anomaly (Internal Softening): The slag-based reference (H15) exhibited inconsistent mass preservation. Because the silica-rich gel produced by slag hydration inherently resists acid dissolution [19], the specimen maintained its physical weight and geometric profile. However, mechanical tests indicate the acid successfully penetrated the matrix, likely decalcifying the C-S-H gel and causing extensive internal softening. This explains why H15 visually appeared stable while suffering severe structural failure.
- Erosion-Dominated Survival: Conversely, the H10 mixtures experienced rapid dissolution of the outer cement paste, leading to higher mass loss. However, this rapid surface erosion acted sacrificially. Mechanical testing proved that this surface loss protected the inner core, allowing H10 to retain an extraordinary residual flexural strength.
- Mass Discrepancies in Sewage Environments: The notable divergence of the gravimetric metric occurred in the raw sewage environment. The observed mass gains were inconsistent with the expected erosion. This aligns with microbial colonization where a dense, organic biofilm coupled with a soft gypsum-sludge layer accumulates on the concrete surface, masking the underlying chemical attack [4,20].
- The variability observed in the standard deviation (SD) of the mass loss data serves as an indicator of the physical-mechanical interactions at play. Because the prismatic specimens were sectioned from larger cubes, the 'wall effect' was eliminated, and the internal aggregate–paste interface—the Interfacial Transition Zone (ITZ)—was exposed directly to the acid. In mixtures with lower internal cohesion, the acid-induced neutralization of the paste at the ITZ allowed for the mechanical shedding of coarse aggregates, or 'aggregate fallout.' This phenomenon, which contributes to higher SD

numbers in certain high-replacement blends, provides a more realistic representation of sewer pipe erosion where high flow velocities and grit continuously strip away weakened material. Consequently, a high SD in this study is not viewed as an experimental liability but as an observation of non-uniform failure, stochastic failure within the concrete matrix, further emphasizing that mass loss measurements are influenced by physical shedding that may not correlate with the remaining core's integrity.

6.2. Mechanisms of Enhanced Structural Survival

The superior structural retention of the Metakaolin-optimized (H22) and matured cyment (H11) blends can be attributed to two distinct but complementary defence mechanisms:

- Physical Densification: The H10 mix achieved high residual strength due to a profound physical filler effect. It is hypothesized that the ultra-fine particles of the mechanically activated volcanic tuff tightly packed the interstitial capillary voids. This potential densification would create a highly tortuous pore network that restricts the inward diffusion of sulphate and hydrogen ions.
- Chemical Starvation: The Metakaolin-optimized mixtures (H22) utilized an active chemical defence. Sulfuric acid attack primarily targets Calcium Hydroxide (Portlandite). The inclusion of hyper-reactive Metakaolin consumed the available Portlandite during the hydration phase via the pozzolanic reaction [8,11]. By converting the vulnerable free lime into stable secondary C-S-H gel before exposure, the matrix appears to effectively "starve" the acid of its primary reactant.

6.3. Methodological Limitations

A limitation of this experimental program is the intentional variation in water-to-cement (w/c) ratios, superplasticizer (PCE) dosages, and resultant fresh flow classes across the 27 mix designs. Because the supplementary cementitious materials utilized—specifically the flash-calcined metakaolin and mechanically activated volcanic tuff—possess specific surface areas exponentially higher than the reference CEM I, holding the w/c ratio and PCE dosage constant across all mixtures was practically infeasible. Enforcing a strict single-variable control would have resulted in unworkable, un-compactable mixtures for the high-fines blends, or severe segregation and bleeding in the reference blends. Consequently, the mix design strategy prioritized achieving a comparable, practically viable fresh state (targeting F3/F4 consistencies) to ensure uniform compaction and minimize macro-defect formation. While this approach accurately reflects industry-standard proportioning practices for high-performance concrete, it introduces multi-variable complexity that makes isolating the purely chemical effect of the binder alone more challenging.

Furthermore, a recognized limitation of this experimental protocol is the intentional variation in handling and cleaning procedures across the different exposure environments. The 5% H_2SO_4 brushed group was subjected to mechanical scrubbing to simulate the highly turbulent, erosive hydrodynamic conditions often found at the invert of sewer pipes, where high flow velocities and suspended grit continuously strip away protective reaction products. Conversely, the static 1% H_2SO_4 and raw sewage groups were deliberately handled with low-impact methods (gentle rinsing and SSD drying) to simulate the low-flow or stagnant conditions typical of the sewer crown. This approach allowed for the observation of natural gypsum diffusion barriers and organic biofilm accumulation.

Because these handling methods actively alter the specimen surface, a direct, one-to-one quantitative comparison of mass change between the different exposure groups must be interpreted with caution. However, this methodological variance highlights the central thesis of this research. Real-world wastewater infrastructure is subjected to vastly different hydrodynamic forces. Since environmental flow dynamics heavily dictate surface mass

retention, gravimetric measurements become an inconsistent metric for overall structural durability. The utilization of residual flexural strength as the primary performance indicator effectively bypasses these surface-level handling variations, providing a universal, comparable measure of internal matrix integrity regardless of the erosive environment.

While the experimental protocol evaluated individual specimens in triplicate to establish intra-batch variability (standard deviation), independent inter-batch replications for each of the 27 mix designs were not conducted due to the extensive scope of the test matrix. To mitigate this limitation and ensure the reliability of the findings, the experimental design utilized a parametric approach. The consistency of the observed degradation trends—specifically the distinct phenomenological behaviours of the three additives (metakaolin, silica fume, and volcanic tuff) across multiple replacement ratios and w/c configurations—serves to internally validate the primary mechanisms proposed in this study.

7. Conclusions

This study investigated the durability of high-performance concrete blends in aggressive biogenic and chemical wastewater environments. Based on the evaluation of mix designs exposed to 5% H_2SO_4, 1% H_2SO_4, and raw sewage, the following conclusions are drawn:

1. Mass Loss Requires Complementary Data: Gravimetric mass loss alone may not fully reflect structural survival. The slag-based reference (H15) exhibited excellent mass preservation (losing only 19.17% at 56 days) but suffered severe reduction in load-bearing capacity (76.0% retention) due to suspected internal decalcification.
2. The Sewage Anomaly: In raw sewage, mass loss measurements were rendered invalid by a "negative erosion" phenomenon (+1.21% mass gain for reference mixes) caused by liquid absorption and organic biofilm clogging, which masked the chemical attack proven by active pH neutralization data.
3. Structural Integrity of Optimized Blends: Binary blends incorporating matured cyment (H10) demonstrated exceptional durability, retaining up to 11.28 MPa (92.7% retention) in extreme 5% acid. This performance is attributed to physical densification and the pozzolanic conversion of free lime, which chemically "starved" the acid reaction.
4. Novelty of Specimen Preparation: By utilizing saw-cut specimens to intentionally expose the ITZ and aggregate–paste interface, this study provides a more rigorous benchmark for structural survivability. The identification of 'aggregate fallout' as a driver for data variability highlights a physical degradation pathway that is frequently obscured by the smooth, cast surfaces typically used in standardized acid tests.
5. Requirement for Complementary Mechanical Testing: Current standards relying solely on mass loss may overlook internal capacity reduction in cements that remain geometrically intact. Future testing protocols should incorporate Residual Flexural Strength Testing alongside gravimetric analysis to provide a holistic evaluation of true load-bearing survivability.

Author Contributions: H.A.: Conceptualization, Methodology, Software, Investigation, Writing—Original Draft; S.G.N.: Supervision, Writing—Review and Editing. All authors have read and agreed to the published version of the manuscript.

Funding: This research received no external funding.

Data Availability Statement: The original data presented in the study are openly available in FigShare at https://doi.org/10.6084/m9.figshare.32149183.

Conflicts of Interest: The authors declare no conflicts of interest.

References

1. Kaempfer, W.; Berndt, M. Polymer modified mortar with high resistance to acid corrosion by biogenic sulfuric acid. In Proceedings of the 11th ICPIC Congress, Berlin, Germany, 2–4 June 2004.
2. Grengg, C.; Mittermayr, F.; Ukrainczyk, N.; Koraimann, G.; Kienesberger, S.; Dietzel, M. Advances in concrete materials for sewer systems affected by microbial induced concrete corrosion: A review. *Water Res.* **2018**, *134*, 341–352. [CrossRef] [PubMed]
3. Monteny, J.; Vincke, E.; Beeldens, A.; De Belie, N.; Taerwe, L.; Verstraete, W. Chemical, microbiological, and in situ test methods for biogenic sulfuric acid corrosion of concrete. *Cem. Concr. Res.* **2000**, *30*, 623–634. [CrossRef]
4. Alexander, M.; Fourie, C. Performance controls for concrete in aggressive environments. *Constr. Build. Mater.* **2011**, *25*, 638–644.
5. *CEN. EN 206:2013+A1:2016*; Concrete–Specification, Performance, Production and Conformity. European Committee for Standardization: Brussels, Belgium, 2016.
6. *ASTM C267-20*; Standard Test Methods for Chemical Resistance of Mortars, Grouts, and Monolithic Surfacings and Polymer Concretes. ASTM International: West Conshohocken, PA, USA, 2020.
7. Scrivener, K.; De Belie, N. Bacteriogenic sulfuric acid attack of cementitious materials in sewage systems. *RILEM Tech. Lett.* **2016**, *1*, 69–74.
8. Lloyd, R.R.; Provis, J.L.; Devis, J.S. Acid resistance of inorganic polymer binders. 1. Corrosion rate. *Ind. Eng. Chem. Res.* **2012**, *51*, 12648–12658. [CrossRef]
9. Beddoe, R.E.; Dorner, H.W. Modelling acid attack on concrete: Part I. The essential mechanisms. *Cem. Concr. Res.* **2005**, *35*, 2333–2339. [CrossRef]
10. Zivica, V.; Bajza, A. Acidic attack of cement based materials—A review. Part 2. Factors of influence. *Constr. Build. Mater.* **2002**, *16*, 215–222. [CrossRef]
11. Allahverdi, A.; Škvára, F. Sulfuric acid attack on hardened paste of geopolymer cements. Part 1. Mechanism of corrosion at relatively high concentrations. *Ceram.-Silikáty* **2005**, *49*, 225–229.
12. Islander, R.L.; Devinny, J.S.; Mansfeld, F.; Postyn, A.; Shih, H. Microbial ecology of crown corrosion in sewers. *J. Environ. Eng.* **1991**, *117*, 751–770. [CrossRef]
13. Roberts, D.J.; Nica, D.; Zuo, G.; Davis, J.L. Quantifying microbially induced deterioration of concrete: Initial studies. *Int. Biodeterior. Biodegrad.* **2002**, *49*, 227–234. [CrossRef]
14. Jiang, G.; Keller, J.; Bond, P.L.; Yuan, Z. Microbial influenced concrete corrosion in the urban wastewater system: A review. *Water Res.* **2020**, *187*, 116434.
15. Wells, T.; Melchers, R.E. Modelling concrete deterioration in sewers using theory and field observations. *Cem. Concr. Res.* **2015**, *77*, 82–96. [CrossRef]
16. Alexander, M.; Beushausen, H. Durability, service life prediction, and modelling for reinforced concrete structures–review and critique. *Cem. Concr. Res.* **2019**, *122*, 17–29. [CrossRef]
17. Chaudhari, B.; Panda, B.; Šavija, B.; Chandra Paul, S. Microbiologically Induced Concrete Corrosion: A Concise Review of Assessment Methods, Effects, and Corrosion-Resistant Coating Materials. *Materials* **2022**, *15*, 4279. [CrossRef] [PubMed]
18. Bakera, A.T.; Aboulela, A.; Alexander, M.G.; Bertron, A.; Peyre Lavigne, M.; Meulenyzer, S.; Patapy, C. Performance of Sewer Concretes with Calcium Sulpho-Aluminate Cement and Portland Cement Blends: Field and Laboratory Studies. *Materials* **2025**, *18*, 1256. [CrossRef] [PubMed]
19. Aiken, T.A.; Russell, M.; Macphee, D.E. Microstructural interactions in slag-blended cements under sulfuric acid attack. *Cem. Concr. Res.* **2018**, *105*, 54–63.
20. Godinho, J.P.; Medeiros, M.H.F.; Neto, A.M.; Lima, V.M.E.; De Souza, D.J. Laboratory-field assessment of concrete exposed to biogenic sulphuric acid: Influence of SCM-based binders on long-term degradation. *Constr. Build. Mater.* **2025**, *493*, 143185. [CrossRef]

Disclaimer/Publisher's Note: The statements, opinions and data contained in all publications are solely those of the individual author(s) and contributor(s) and not of MDPI and/or the editor(s). MDPI and/or the editor(s) disclaim responsibility for any injury to people or property resulting from any ideas, methods, instructions or products referred to in the content.